PHYSICAL REVIEW D, VOLUME 70, 053007

Pion form factor in the k_T factorization formalism

Tao Huang,[1,2,*] Xing-Gang Wu,[2,†] and Xing-Hua Wu[2,‡]

[1]*CCAST (World Laboratory), P.O. Box 8730, Beijing 100080, People's Republic of China*

[2]*Institute of High Energy Physics, Chinese Academy of Sciences, P.O. Box 918(4), Beijing 100039, China.*

(Received 21 April 2004; revised manuscript received 20 July 2004; published 15 September 2004)

Based on the light-cone (LC) framework and the k_T factorization formalism, the transverse momentum effects and the different helicity components' contributions to the pion form factor $F_\pi(Q^2)$ are recalculated. In particular, the contributions to the pion form factor from the higher-helicity components ($\lambda_1 + \lambda_2 = \pm 1$), which come from the spin-space Wigner rotation, are analyzed in the soft and hard energy regions, respectively. Our numerical results show that the right power behavior of the hard contribution from the higher-helicity components can only be obtained by fully keeping the k_T dependence in the hard amplitude, and that the k_T dependence in LC wave function affects the hard and soft contributions substantially. As an example, we employ a model LC wave function to calculate the pion form factor and then compare the numerical predictions with the experimental data.

DOI: 10.1103/PhysRevD.70.053007 PACS numbers: 13.40.Gp, 12.38.Bx, 12.39.Ki

I. INTRODUCTION

In the perturbative QCD (PQCD) theory, the hadronic distribution amplitude (DA) and the structure function that enter exclusive and inclusive processes via the factorization theorem at high momentum transfer can be determined by the hadronic wave function, and therefore they are the underlying links between hadronic phenomena in QCD at large distance (nonperturbative) and small distance (perturbative). However we require a conceptual framework within which the connection between the hadron and its constituents can be made precise. A particularly convenient and intuitive framework is based upon the Fock-state decomposition of hadronic state, which arises naturally in the "light-cone quantization" [1,2]. A light-cone (LC) wave function is a localized stationary solution of the LC Schrödinger equation that describes the evolution of a state $|\Psi(\tau)\rangle$ on the LC time $\tau \equiv x^+ = (x^0 + x^3)$ in physical LC gauge $A^+ = (A^0 + A^3) = 0$, i.e., $i\partial_\tau|\Psi(\tau)\rangle = H_{\rm LC}|\Psi(\tau)\rangle$, where $H_{\rm LC} \equiv P^- = (P^0 - P^3)$ is the LC Hamiltonian. The LC wave function is the amplitude $\Psi_n(x_i, \mathbf{k}_{\perp i}, \lambda_i)$ to find n particles (quarks, antiquarks, and gluons) with momenta $k_i = (x_i, \mathbf{k}_{\perp i})$ in a pion of momentum P, where $x_i = k_i^+/P^+$ ($\sum_i x_i = 1$), is the LC momentum fraction of the ith (anti)quark or gluon in the n-particle Fock-state.

An important issue, which has to be addressed when applying PQCD to exclusive processes, is how to implement factorization, i.e., how to separate perturbative contributions from those intrinsic to the bound-state wave functions. The k_T factorization is one of the fundamental tools of PQCD. Since the k_T factorization theorem has been proposed [1–3], it has been widely applied to various processes. Until recently, a better proof of the k_T factorization theorem for exclusive processes in PQCD has been provided by M. Nagashima and H. N. Li [4]. Their starting point is that the on-shell valence partons carry longitudinal momenta initially, and then acquire k_T through collinear gluon exchanges before participating in hard-scattering. A hard amplitude, derived from the parton level amplitude with gauge-invariant and infrared divergent meson wave function being subtracted, is then gauge invariant and infrared finite. This way, they demonstrated that all the physical quantities from the k_T factorization theorem are gauge-invariant. Therefore for the pion form factor, when in the energy region that PQCD is applicable, we can take the following factorization formula [1,3,5–7],

$$F_\pi(Q^2) = \sum_{n,m,\lambda_{i,j}} \int [dx_i d\mathbf{k}_{i\perp}]_n [dy_j d\mathbf{l}_{j\perp}]_m \times \Psi_n^*(x_i, \mathbf{k}_{i\perp}, \lambda_i; \mu) T_{nm}(x_i, \mathbf{k}_{i\perp}; y_j, \mathbf{l}_{j\perp}; \mathbf{q}_{i\perp}; \mu) \times \Psi(y_j, \mathbf{l}_{j\perp}, \lambda_j; \mu) \tag{1}$$

where the summation is over all helicities (λ_i, λ_j) and n, m extends over the low momentum states only, and $T_{n,m}$ are the partonic matrix elements of the effective current operator. μ is the energy scale separating the perturbative region from the nonperturbative region, and in order for the perturbative approach to make sense, μ has to be much larger than $\Lambda_{\rm QCD}$ so that $\alpha_s(\mu)$ is small.

It is well known that the numerical predictions for the pion form factor from only the leading order are much smaller than the experimental data. In order to short the gap between the experimental data and the theoretical predications, two ways are tried in literature, one is to consider the nonperturbative contributions (see examples in Refs. [8–15]); the other is to consider the nonleading order contributions, which come from the higher-twist effect [16], the higher order in α_s [17], the higher Fock states [5], the higher-helicity components in the LC wave

*Electronic address: huangtao@mail.ihep.ac.cn
†Electronic address: wuxg@mail.ihep.ac.cn
‡Electronic address: xhwu@mail.ihep.ac.cn

function [7,18,19], etc. As has been pointed out in Refs. [7,18,19], the higher-helicity components in the LC wave function might provide a great contribution to the pion form factor at the present experimentally accessible energy region. However, the conclusions are conflicting in those references. In Refs. [18], the authors pointed out a large *enhancement* to the usual-helicity component's contribution, while in Ref. [19], based on the modified PQCD approach [3] and by neglecting the transverse momentum dependence in the quark propagator, a great *suppression* has been observed. And in Ref. [7], they pointed out that the higher-helicity contribution is of order $1/Q^4$, but only a qualitative discussion was given there. It is then necessary to clarify the present situation.

In the present paper, we recalculate all the helicity components' contributions to the pion form factor within the LC PQCD framework, which is consistent with the using of LC wave function. Our calculation keeps the transverse momentum dependence fully in the hard-scattering amplitude, i.e., such dependence is kept in both the quark propagator and the gluon propagator, and the resultant expression gives the right power behavior of the hard contribution from the higher-helicity components as Q^2 goes to large energy region. Furthermore, we carry out the numerical calculations for the hard and the soft parts of all the helicity components' contributions. In order to explain our picture and to clarify the difference between Ref. [18] and Ref. [19], we employ a model LC wave function with reasonable constraints. We show that it is substantial to take k_T dependence in the wave function into account and to keep the transverse momentum dependence in the quark propagator in the k_T factorization formalism within the LC framework.

The purpose of this paper is to reanalyze the effects coming from the higher-helicity components of the pion wave function within the framework of LC PQCD and the k_T factorization formalism, then give a comparative study on the contributions from different helicity components within the soft and the hard region, respectively. In Sec. II, based on the k_T factorization formula, the hard-scattering amplitude is given within the LC framework. In Sec. III, with a model LC wave function, the hard contributions from different helicity components of pion are analyzed. Section IV is devoted to give a discussion of the soft part contribution, especially on the contributions from different helicity components. A conclusion and a brief summary are presented in the final section.

II. HARD-SCATTERING AMPLITUDE WITH K_T DEPENDENCE

The hard-scattering amplitude for the higher-helicity components $(\lambda_1+\lambda_2=\pm1)$ of the LC wave function within the LC PQCD approach has been given in Ref. [7]. In Ref. [7], with a simple argument that when summing over all the helicity states only the real part of each hard-scattering amplitude survives, they used a simplified combined expression for the hard-scattering amplitude [Eq. (20) there] at the very beginning. Since the combination of the imaginary part from both the spin-space wave function and the hard kernel can also make contributions, it is not a strict argument and can only be true under some proper approximations. In the present section, we will not do such simplifications in our calculation and will give the hard-scattering amplitude for all the helicity components that come from the spin-space Wigner rotation. So even though some of our present procedures are the same as those of Ref. [7], we will put all the necessary ones here for self-consistence.

In the LC quantization, at higher momentum transfer, the hard contribution to the pion form factor can be written as [3,6,7,18]

$$\begin{aligned}F_\pi(Q^2) = \int&[dx][dy][d^2\mathbf{k}_\perp][d^2\mathbf{l}_\perp]\Psi^{*(1-x)Q}(x,\mathbf{k}_\perp,\lambda)\\&\times T_H(x,y,\mathbf{q}_\perp,\mathbf{k}_\perp,\mathbf{l}_\perp,\lambda,\lambda')\Psi^{(1-y)Q}(y,\mathbf{l}_\perp,\lambda')\\&+\cdots,\end{aligned}\qquad(2)$$

where the ellipses represent the higher Fock-state contributions, $[dx]=dx_1dx_2\delta(1-x_1-x_2)$ and $[d^2\mathbf{k}_\perp]=d^2\mathbf{k}_\perp/16\pi^3$. $\Psi^{[(1-x)Q]}(x,\mathbf{k}_\perp,\lambda)$ is the valence Fock-state LC wave function with helicity λ and with a cutoff on $|\mathbf{k}_\perp|$ that is of order $(1-x)Q$. Such a cutoff on $|\mathbf{k}_\perp|$ is necessary to insure that the wave function is only responsible for the lower momentum region. T_H contains all two-particle irreducible amplitudes for $\gamma^*+q\bar{q}\to q\bar{q}$ and should be calculated from the time-ordered diagrams in LC PQCD. In the LC gauge, the nominal power law contribution to $F_\pi(Q^2)$ as $Q\to\infty$ is $F_\pi(Q^2)\sim 1/(Q^2)^{n-1}$ [20], under the condition that n quark or gluon constituents are forced to change direction. Thus only the $q\bar{q}$ component of $\psi^{[(1-x)Q]}(x,\mathbf{k}_\perp,\lambda)$ contributes at the leading $1/Q^2$.

The lowest-order contribution for the hard-scattering amplitude T_H comes from the one-gluon exchange shown in Fig. 1. To simplify our notations, we separate the spin-space wave function $\chi^K(x,\mathbf{k}_\perp,\lambda)$ out from the whole LC wave function, i.e., $\psi^{(1-x)Q}(x,\mathbf{k}_\perp,\lambda)\to\chi^K(x,\mathbf{k}_\perp,\lambda)\varphi^{(1-x)Q}(x,\mathbf{k}_\perp,\lambda)$ and then combined the spin-space wave function $\chi^K(x,\mathbf{k}_\perp,\lambda)$ into the original T_H to form a new one, i.e.,

$$\begin{aligned}T_H = \xi_1T_H^{(\lambda_1+\lambda_2=0)}(\uparrow\downarrow\to\uparrow\downarrow)+\xi_1T_H^{(\lambda_1+\lambda_2=0)}(\downarrow\uparrow\to\downarrow\uparrow)\\+\xi_2T_H^{(\lambda_1+\lambda_2=1)}(\uparrow\uparrow\to\uparrow\uparrow)+\xi_2^*T_H^{(\lambda_1+\lambda_2=-1)}(\downarrow\downarrow\to\downarrow\downarrow),\end{aligned}\qquad(3)$$

where $\lambda_{1,2}$ are the helicities for the (initial or final) pion's two constitutent quarks, respectively,

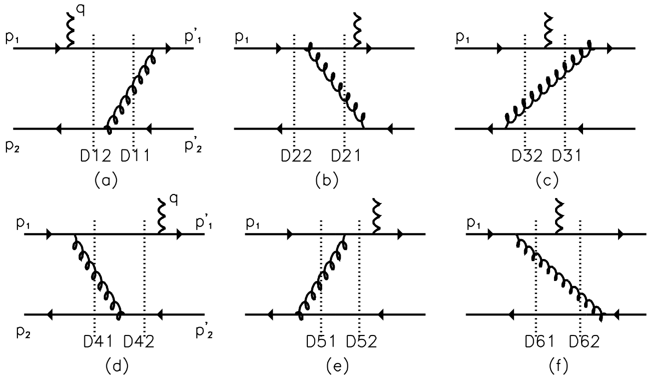

FIG. 1. Six leading order time-ordered Feynman diagrams for the hard-scattering amplitude, where $p_1 = (x_1, \mathbf{k}_\perp)$, $p_2 = (x_2, -\mathbf{k}_\perp)$, $p'_1 = (y_1, y_1\mathbf{q}_\perp + \mathbf{l}_\perp)$, $p'_2 = (y_2, y_2\mathbf{q}_\perp - \mathbf{l}_\perp)$.

$\xi_1 = \frac{m^2}{2[m^2+\mathbf{k}_\perp^2]^{1/2}[m^2+\mathbf{l}_\perp^2]^{1/2}}$ and $\xi_2 = \frac{\mathbf{k}_\perp\cdot\mathbf{l}_\perp + i(\mathbf{k}_\perp\times\mathbf{l}_\perp)}{2[m^2+\mathbf{k}_\perp^2]^{1/2}[m^2+\mathbf{l}_\perp^2]^{1/2}}$ are two coefficients derived from $\chi^K(x, \mathbf{k}_\perp, \lambda)$. Equation (3) is different from Eq. (20) in Ref. [7], and one may observe that if combining the imaginary part of ξ_2 that comes form the higher-helicity spin-space wave function with the imaginary part of the hard kernel $T_H^{(\lambda_1+\lambda_2=\pm1)}$, it can make real contribution to T_H. The spin-space wave function $\chi^K(x, \mathbf{k}_\perp, \lambda)$ can be found in Ref. [21]. In Eq. (3) there is no hard-scattering amplitude with quark and antiquark helicities being changed due to the fact that the quark helicity is conserved at each quark-gluon (or photon)-quark vertex in the limit of vanishing quark mass [2].

To simplify the hard-scattering amplitude, we adopt the standard momentum assignment at the “infinite-momentum” frame [2],

$$P_\pi = (P^+, P^-, \mathbf{P}_\perp) = (1, 0, \mathbf{0}_\perp), \qquad q = (0, \mathbf{q}_\perp^2, \mathbf{q}_\perp), \tag{4}$$

where P^+ is arbitrary because of Lorentz invariance and the momentum transfer $Q^2 = -q^2 = \mathbf{q}_\perp^2$. Using D to denote the “energy-denominator” in the six Feynman diagrams (x^+-ordered diagrams), all the needed “energy-denominators” can be found in Ref. [7]. With the help of the above equations, the hard-scattering amplitude can be shortly expressed as,

$$T_H^{(\lambda_1+\lambda_2)} = g^2 C_F[T_a^{(\lambda_1+\lambda_2)} + T_b^{(\lambda_1+\lambda_2)} + T_c^{(\lambda_1+\lambda_2)}] + \left\{ \begin{matrix} x \leftrightarrow y \\ \mathbf{k}_\perp \leftrightarrow -\mathbf{l}_\perp \end{matrix} \right\}, \tag{5}$$

where the three terms in the parentheses, which correspond to Fig. 1(a)–1(c), respectively, can be written as

$$\begin{aligned} T_a^{(\lambda_1+\lambda_2)} &= \frac{N^{(\lambda_1+\lambda_2)}}{D_{11}D_{12}} \frac{\theta(y_1 - x_1)}{y_1 - x_1} + T_a^{\mathrm{in}}, \\ T_a^{\mathrm{in}} &= -\frac{4}{D_{12}} \frac{\theta(y_1 - x_1)}{(y_1 - x_1)^2}, \end{aligned} \tag{6}$$

$$\begin{aligned} T_b^{(\lambda_1+\lambda_2)} &= \frac{N^{(\lambda_1+\lambda_2)}}{D_{21}D_{22}} \frac{\theta(x_1 - y_1)}{x_1 - y_1} + T_b^{\mathrm{in}}, \\ T_b^{\mathrm{in}} &= -\frac{4}{D_{22}} \frac{\theta(x_1 - y_1)}{(y_1 - x_1)^2}, \end{aligned} \tag{7}$$

$$T_c^{(\lambda_1+\lambda_2)} = \frac{N^{(\lambda_1+\lambda_2)}}{D_{31}D_{32}} \frac{\theta(y_1 - x_1)}{y_1 - x_1}. \tag{8}$$

Here T_a^{in} and T_b^{in} represent the contributions from the instantaneous diagrams in the LC PQCD. The numerator $N^{(\lambda_1+\lambda_2)}$ for the usual-helicity components ($\lambda_1 + \lambda_2 = 0$) can be written as

$$\begin{aligned} N^{(\lambda_1+\lambda_2=0)} = &-\mathbf{q}_\perp^2\left[\frac{x_2(x_1x_2 + y_1y_2)}{x_1(y_1 - x_1)^2}\right] - \mathbf{k}_\perp^2\left[\frac{(x_1x_2 + y_1y_2)}{x_1x_2(y_1 - x_1)^2}\right] - \mathbf{l}_\perp^2\left[\frac{(x_1x_2 + y_1y_2)}{y_1y_2(y_1 - x_1)^2}\right] - (2\mathbf{q}_\perp\cdot\mathbf{k}_\perp)\left[\frac{(x_1x_2 + y_1y_2)}{x_1(y_1 - x_1)^2}\right] \\ &+(\mathbf{q}_\perp\cdot\mathbf{l}_\perp)\left[\frac{(x_1x_2 + y_1y_2)(x_2y_1 + x_1y_2)}{x_1y_1y_2(y_1 - x_1)^2}\right] + (\mathbf{k}_\perp\cdot\mathbf{l}_\perp)\left[\frac{(x_1x_2 + y_1y_2)(x_2y_1 + x_1y_2)}{x_1x_2y_1y_2(y_1 - x_1)^2}\right] \\ &\pm i\left[\frac{(x_2 - y_1)(\mathbf{l}_\perp \times [\mathbf{k}_\perp + x_2\mathbf{q}_\perp])}{x_1x_2y_1y_2}\right], \end{aligned} \tag{9}$$

where the plus sign corresponds to (↑↓→↑↓) and the minus sign corresponds to (↓↑→↓↑). And for the higher-helicity components ($\lambda_1 + \lambda_2 = \pm1$),

$$\begin{aligned} N^{(\lambda_1+\lambda_2=\pm1)} = &-\mathbf{q}_\perp^2\left[\frac{x_2(x_2y_1 + x_1y_2)}{x_1(y_1 - x_1)^2}\right] - \mathbf{k}_\perp^2\left[\frac{(x_2y_1 + x_1y_2)}{x_1x_2(y_1 - x_1)^2}\right] - \mathbf{l}_\perp^2\left[\frac{(x_2y_1 + x_1y_2)}{y_1y_2(y_1 - x_1)^2}\right] - (2\mathbf{q}_\perp\cdot\mathbf{k}_\perp)\left[\frac{(x_2y_1 + x_1y_2)}{x_1(y_1 - x_1)^2}\right] \\ &+(\mathbf{q}_\perp\cdot\mathbf{l}_\perp)\left[\frac{(x_2y_1 + x_1y_2)^2}{x_1y_1y_2(y_1 - x_1)^2}\right] + (\mathbf{k}_\perp\cdot\mathbf{l}_\perp)\left[\frac{(x_2y_1 + x_1y_2)^2}{x_1x_2y_1y_2(y_1 - x_1)^2}\right] \pm i\left[\frac{\mathbf{l}_\perp \times (\mathbf{k}_\perp + x_2\mathbf{q}_\perp)}{x_1x_2y_1y_2}\right], \end{aligned} \tag{10}$$

where the plus sign corresponds to $\lambda_1 + \lambda_2 = 1$ (↑↑→↑↑) and the minus sign corresponds to $\lambda_1 + \lambda_2 = -1$ (↓↓→↓↓). The first terms in the above two equations give the ordinary leading $1/Q^2$ contributions.

To simplify the hard-scattering amplitude, we adopt the same two prescriptions as have been described in Ref. [7]: (1) The terms proportional to the “bound energies” of the pion, i.e., $\sim\mathbf{k}_\perp^2/(x_1x_2)$ and $\sim\mathbf{l}_\perp^2/(y_1y_2)$ can be ignored to avoid the involvement of the higher Fock states contributions [6]. (2) The terms such as $\mathbf{k}_\perp^2/\mathbf{q}_\perp^2$ and $\mathbf{l}_\perp^2/\mathbf{q}_\perp^2$ in both the "energy-denominators" and the numerator $N^{(\lambda_1+\lambda_2)}$ can be neglected due to the fact that $\mathbf{k}_\perp^2 \ll \mathbf{q}_\perp^2$ and $\mathbf{l}_\perp^2 \ll \mathbf{q}_\perp^2$. Furthermore, as has been pointed out in Refs. [6,22], the natural variable to make a separation of perturbative contribution from that intrinsic to the bound-state wave function is the LC energy in the LC perturbative expansion. Under such conditions, the two energy flow $\left[-\frac{(x_2\mathbf{q}_\perp+\mathbf{k}_\perp)^2}{x_1x_2}\right]$ and $\left[-\frac{[y_2(x_2\mathbf{q}_\perp+\mathbf{k}_\perp)-x_2\mathbf{l}_\perp]^2}{x_2y_2(y_1-x_1)}\right]$ in the gluon propagator should be large, otherwise we cannot apply the PQCD, i.e.,

$$(x_2\mathbf{q}_\perp + \mathbf{k}_\perp)^2 \gg \langle \mathbf{k}_\perp^2 \rangle \sim \bar{\Lambda}^2$$

and

$$[y_2(x_2\mathbf{q}_\perp + \mathbf{k}_\perp) - x_2\mathbf{l}_\perp]^2 \gg \langle \mathbf{k}_\perp^2 \rangle, \qquad \langle \mathbf{l}_\perp^2 \rangle \sim \bar{\Lambda}^2$$

are two extra conditions which make the PQCD applicable, where $\bar{\Lambda}$, being of $\mathcal{O}(\Lambda_{QCD})$, represents a hadronic scale.

With the above prescriptions, we finally obtain

$$T_H = T_H^{(\lambda_1+\lambda_2=0)} + T_H^{(\lambda_1+\lambda_2=\pm 1)} \tag{11}$$

with

$$\begin{aligned} T_H^{(\lambda_1+\lambda_2=0)} = {} & \frac{16\xi_1 \pi C_F \alpha_s(Q^2)}{(1-x)(1-y)xy} \{[(x-1)\mathbf{q}_\perp^2 - 2\mathbf{k}_\perp \cdot \mathbf{q}_\perp][2\mathbf{l}_\perp \cdot \mathbf{q}_\perp + (y-1)\mathbf{q}_\perp^2]\}^{-1}\{(x-1)[2\mathbf{l}_\perp \cdot \mathbf{q}_\perp + (y-1)\mathbf{q}_\perp^2] \\ & -2(y-1)\mathbf{k}_\perp \cdot \mathbf{q}_\perp\}^{-1}(2(y-1)y[1-y+x(2y-1)](\mathbf{k}_\perp \cdot \mathbf{q}_\perp)^2 + (x-1)x[2\mathbf{l}_\perp \cdot \mathbf{q}_\perp + (y-1)\mathbf{q}_\perp^2] \\ & \times\{[1-y+x(2y-1)](\mathbf{l}_\perp \cdot \mathbf{q}_\perp) + 2(x-1)(y-1)y\mathbf{q}_\perp^2\} - (x-1)(y-1)y(\mathbf{k}_\perp \cdot \mathbf{q}_\perp) \\ & \times\{8x(\mathbf{l}_\perp \cdot \mathbf{q}_\perp) + [1-y+x(6y-5)]\mathbf{q}_\perp^2\}), \end{aligned} \tag{12}$$

and

$$\begin{aligned} T_H^{(\lambda_1+\lambda_2=\pm 1)} = {} & \frac{8(\xi_2+\xi_2^*)\pi A^2 C_F \alpha_s(Q^2)}{(1-x)(1-y)xy} \{[(x-1)\mathbf{q}_\perp^2 - 2\mathbf{k}_\perp \cdot \mathbf{q}_\perp][2\mathbf{l}_\perp \cdot \mathbf{q}_\perp + (y-1)\mathbf{q}_\perp^2]\}^{-1} \\ & \times\{(x-1)[2\mathbf{l}_\perp \cdot \mathbf{q}_\perp + (y-1)\mathbf{q}_\perp^2] - 2(y-1)\mathbf{k}_\perp \cdot \mathbf{q}_\perp\}^{-1}(2(x-1)x(\mathbf{l}_\perp \cdot \mathbf{q}_\perp)^2 + (y-1) \\ & \times\{2y(\mathbf{k}_\perp \cdot \mathbf{q}_\perp)^2 + (x-1)[x(\mathbf{l}_\perp \cdot \mathbf{q}_\perp) - y(\mathbf{k}_\perp \cdot \mathbf{q}_\perp)]\mathbf{q}_\perp^2\}). \end{aligned} \tag{13}$$

From Eq. (13), one may observe that the net contribution from the imaginary part of the higher-helicity LC wave function contributes zero, but only under the above two prescriptions can we draw such a conclusion. After doing a simple transformation, one may find Eq. (13) coincides well with the one obtained in Ref. [7]. The hard-scattering amplitude Eq. (12) for the usual-helicity components ($\lambda_1 + \lambda_2 = 0$) is different from others (see, for example, in Ref. [6]) after including all the k_T dependence in the LC PQCD framework. Because of the complicated integral in Eq. (2), Ref. [7] did not give the numerical results for the higher-helicity contribution of the pion form factor. We will apply the VEGAS program [23] to evaluate the hard contributions in the next sections.

III. HARD CONTRIBUTIONS TO THE PION FORM FACTOR

In order to get the hard contributions for the pion form factor from Eq. (2), we need to know the soft hadronic wave function. Several important nonperturbative approaches have been developed to provide the theoretical predictions for the hadronic wave function [15,21,22,24–27]. One useful way is to use the approximate bound-state solution of a hadron in terms of the quark model as the starting point for modelling the hadronic valence wave function. The Brodsky-Huang-Lepage (BHL) prescription [22] of the hadronic wave function is in fact obtained in this way by connecting the equal-time wave function in the rest frame and the wave function in the infinite-momentum frame. In Ref. [21], based on the BHL prescription, a revised LC quark model wave function has been raised that can give both the approximate asymptotic DA and the reasonable valence state structure function which does not exceed the pion structure function data simultaneously. So in the present paper, we will use this revised LC quark model wave function for our latter discussions, i.e.,

$$\begin{aligned} \Psi(x, \mathbf{k}_\perp) &= \varphi_{\rm BHL}(x, \mathbf{k}_\perp)\chi^K(x, \mathbf{k}_\perp) \\ &= A \exp\left[-\frac{\mathbf{k}_\perp^2 + m^2}{8\beta^2 x(1-x)}\right]\chi^K(x, \mathbf{k}_\perp), \end{aligned} \tag{14}$$

with the normalization constant A, the harmonic scale β and the quark mass m to be determined. With the help of the model wave function, from Eq. (2), we can obtain the leading-twist hard part contributions to the pion form factor. From Eq. (12) we obtain the contributions from the usual-helicity components ($\lambda_1 + \lambda_2 = 0$),

$$F_\pi^{(\lambda_1+\lambda_2=0)}(Q^2) = \int dxdy[d^2\mathbf{k}_\perp][d^2\mathbf{l}_\perp]\frac{8\pi A^2\xi_1 C_F\alpha_s(Q^2)}{(1-x)(1-y)xy}\exp\left[-\frac{\frac{m^2+\mathbf{k}_\perp^2}{x(1-x)}+\frac{m^2+\mathbf{l}_\perp^2}{y(1-y)}}{8\beta^2}\right]\left[\frac{x(x+y-2xy-1)}{(1-x)\mathbf{q}_\perp^2+2\mathbf{q}_\perp\cdot\mathbf{k}_\perp} + \frac{y(x+y-2xy-1)}{(1-y)\mathbf{q}_\perp^2-2\mathbf{q}_\perp\cdot\mathbf{l}_\perp} + \frac{x+y-x^2-y^2}{2(1-y)\mathbf{q}_\perp\cdot\mathbf{k}_\perp-2(1-x)\mathbf{q}_\perp\cdot\mathbf{l}_\perp+(1-x)(1-y)\mathbf{q}_\perp^2}\right], \tag{15}$$

and from Eq. (13) we obtain the contributions from higher-helicity components ($\lambda_1+\lambda_2=\pm1$),

$$F_\pi^{(\lambda_1+\lambda_2=\pm1)}(Q^2) = \int dxdy[d^2\mathbf{k}_\perp][d^2\mathbf{l}_\perp]\frac{4\pi A^2(\xi_2+\xi_2^*)C_F\alpha_s(Q^2)}{(1-x)(1-y)xy}\exp\left[-\frac{\frac{m^2+\mathbf{k}_\perp^2}{x(1-x)}+\frac{m^2+\mathbf{l}_\perp^2}{y(1-y)}}{8\beta^2}\right]\left[\frac{-x}{(1-x)\mathbf{q}_\perp^2+2\mathbf{q}_\perp\cdot\mathbf{k}_\perp} + \frac{-y}{(1-y)\mathbf{q}_\perp^2-2\mathbf{q}_\perp\cdot\mathbf{l}_\perp} + \frac{x+y-2xy}{2(1-y)\mathbf{q}_\perp\cdot\mathbf{k}_\perp-2(1-x)\mathbf{q}_\perp\cdot\mathbf{l}_\perp+(1-x)(1-y)\mathbf{q}_\perp^2}\right], \tag{16}$$

By integrating over the azimuth angles for $\mathbf{k}_\perp$ and $\mathbf{l}_\perp$ with the integration formula shown in the Appendix, the above six dimensional integration can be reduced to four dimensional integration, which can then be dealt with by numerical calculation with the help of the VEGAS program.

Integrating over the azimuth angles for $\mathbf{k}_\perp$ and $\mathbf{l}_\perp$, we obtain the contributions from the usual-helicity components ($\lambda_1+\lambda_2=0$),

$$F_\pi^{(\lambda_1+\lambda_2=0)}(Q^2) = \int dxdyd\eta_1 d\eta_2\frac{A^2\xi_1 C_F\alpha_s(Q^2)|\mathbf{k}_\perp||\mathbf{l}_\perp|}{32\pi^3 xy}\exp\left[-\frac{\frac{m^2+|\mathbf{k}_\perp|^2}{x(1-x)}+\frac{m^2+|\mathbf{l}_\perp|^2}{y(1-y)}}{8\beta^2}\right] \times\left[\frac{x(x+y-1-2xy)}{(1-x)\sqrt{1-\eta_1^2}}+\frac{y(x+y-1-2xy)}{(1-y)\sqrt{1-\eta_2^2}}+\frac{x+y-x^2-y^2}{(1-x)(1-y)\sqrt{1-\eta_1^2}\sqrt{1-\eta_2^2}}\right] \tag{17}$$

and the contributions from the higher-helicity components ($\lambda_1+\lambda_2=\pm1$),

$$F_\pi^{(\lambda_1+\lambda_2=\pm1)}(Q^2) = -\int dxdyd\eta_1 d\eta_2\frac{A^2\xi_3 C_F\alpha_s(Q^2)|\mathbf{k}_\perp||\mathbf{l}_\perp|}{64\pi^3 xy}\exp\left[-\frac{\frac{m^2+|\mathbf{k}_\perp|^2}{x(1-x)}+\frac{m^2+|\mathbf{l}_\perp|^2}{y(1-y)}}{8\beta^2}\right] \times\left[(x+y-2xy)\frac{(1-\sqrt{1-\eta_1^2})(1-\sqrt{1-\eta_2^2})}{(1-x)(1-y)\eta_1\eta_2\sqrt{1-\eta_1^2}\sqrt{1-\eta_2^2}}\right], \tag{18}$$

where $\xi_3=\frac{|\mathbf{k}_\perp||\mathbf{l}_\perp|}{[m^2+\mathbf{k}_\perp^2]^{1/2}[m^2+\mathbf{l}_\perp^2]^{1/2}}$, $|\mathbf{k}_\perp|=Q(1-x)\eta_1/2$ and $|\mathbf{l}_\perp|=Q(1-y)\eta_2/2$, with $\eta_{1,2}$ in the range of (0, 1). In Eq. (18), there is an overall minus sign and because the integrand is always positive, we can draw the conclusion that the higher-helicity components will always *suppress* the contributions from the usual-helicity components.

With the help of the LC wave function Eq. (14) and its parameter values shown in Eq. (28), we show the pion form factor with or without the higher-helicity components in Fig. 2. One may observe a large *suppression* comes from the higher-helicity components as compared to the prediction obtained in the original hard-scattering model [18]. This large suppression was obtained by Ref. [19] with a quite different picture. They argued that the transverse momentum in the quark propagator is of small contribution (about 15% [3,28]). And the hard-scattering amplitude, after neglecting the transverse momentum dependence in the quark propagator, was taken to be

$$T_H^{(\lambda_1+\lambda_2=\pm1)} = -T_H^{(\lambda_1+\lambda_2=0)} = -\frac{4g^2C_F}{x_2y_2Q^2+(\mathbf{k}_\perp-\mathbf{l}_\perp)^2} \overset{Q^2\to\infty}{\approx} -\frac{4g^2C_F}{x_2y_2Q^2}+\frac{4g^2C_F(\mathbf{k}_\perp-\mathbf{l}_\perp)^2}{(x_2y_2Q^2)^2}. \tag{19}$$

It can be seen that the asymptotic behaviors ($Q^2\to\infty$) of the higher-helicity states and the usual-helicity states are directly with *opposite* signs and all states make the contribution at the order of $1/Q^2$. However it is not a right argument and it is the transverse momentum dependence in the quark propagator that causes the asymptotic behavior of higher-helicity contribution is of order $1/Q^4$ other than $1/Q^2$. In the present work, we have considered the k_T dependence both in the wave function and in the hard-scattering amplitude consistently within the LC PQCD approach, then our results have a right power behavior for the higher-helicity contributions.

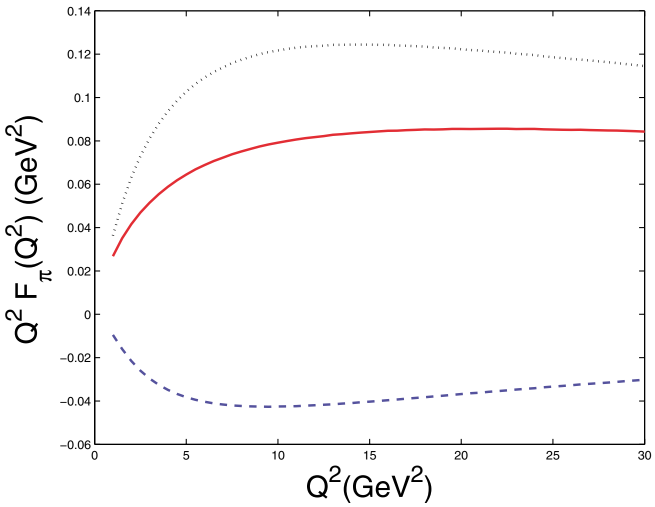

FIG. 2. The hard contribution to the pion form factor $Q^2F_\pi(Q^2)$. The dotted line stands for the contribution from the usual-helicity ($\lambda_1 + \lambda_2 = 0$) components, the dashed line stands for the contribution from the higher-helicity ($\lambda_1 + \lambda_2 = \pm 1$) components and the solid line is the total hard contribution, which is the combined result for all the helicity components.

IV. A DISCUSSION OF THE SOFT CONTRIBUTION TO THE PION FORM FACTOR

In the above sections, we have shown that the inclusion of the higher-helicity components *suppresses* the hard-scattering contributions at moderate Q^2. In order to compare our predictions with the present experimental data, we need to know the contributions from the soft part. Since this part is model-dependent and is still under progress [8–11], as an example, we consider the soft contributions to the pion form factor with the model LC wave function shown in Eq. (14) and study the different helicity components' soft contributions to the pion form factor separately.

For the soft part contribution, we have [29]

$$F^s_{\pi^+}(Q^2) = \int_0^1 dx \int \frac{d^2\mathbf{k}_\perp}{16\pi^3} \sum_{\lambda,\lambda'} \Psi^*(x, \mathbf{k}_\perp, \lambda) \times \Psi(x, \mathbf{k}'_\perp, \lambda') + \cdots, \tag{20}$$

where λ, λ' are the helicities of the wave function, respectively, the first term is the lowest-order contribution from the minimal Fock-state and the ellipses represent those from higher Fock states, which are down by powers of $1/Q^2$ and by powers of α_s.

Taking the LC wave function as is shown in Eq. (14), we obtain

$$F^s_{\pi^+}(Q^2) = \int_0^1 dx \int \frac{d^2\mathbf{k}_\perp}{16\pi^3} \frac{m^2 + \mathbf{k}_\perp \cdot \mathbf{k}'_\perp}{\sqrt{m^2 + \mathbf{k}^2_\perp}\sqrt{m^2 + \mathbf{k}'^2_\perp}} A^2 \times \exp\left[-\frac{\mathbf{k}^2_\perp + m^2}{8\beta^2 x(1-x)} - \frac{\mathbf{k}'^2_\perp + m^2}{8\beta^2 x(1-x)} \right], \tag{21}$$

where $\mathbf{k}'_\perp = \mathbf{k}_\perp + (1-x)\mathbf{q}_\perp$ for the final state LC wave function when taking the Drell-Yan-West assignment [29]. We proceed to integrate the transverse momentum $\mathbf{k}_\perp$ in Eq. (21) with the help of the Schwinger α-representation method,

$$\frac{1}{A^\kappa} = \frac{1}{\Gamma(\kappa)} \int_0^\infty \alpha^{\kappa-1} e^{-\alpha A} d\alpha. \tag{22}$$

Doing the integration over $\mathbf{k}_\perp$, we obtain

$$F^s_{\pi^+}(Q^2) = \int_0^1 dx \int_0^\infty d\lambda \frac{A^2}{128\pi^2(1+\lambda)^3} \exp\left(-\frac{8m^2(1+\lambda)^2 + Q^2(1-x)^2[2+\lambda(4+\lambda)]}{32(1-x)x\beta^2(1+\lambda)} \right) \times \left[I_0\left(\frac{Q^2(x-1)\lambda^2}{32x\beta^2(1+\lambda)} \right) \{32(1-x)x\beta^2(1+\lambda) - Q^2(1-x)^2[2+\lambda(4+\lambda)] + 8m^2(1+\lambda)^2\} - I_1\left(\frac{Q^2(x-1)\lambda^2}{32x\beta^2(1+\lambda)} \right) Q^2(1-x)^2\lambda^2 \right], \tag{23}$$

where the $I_n (n = 0, 1)$ is the modified Bessel function of the first kind. After taking the expansion in the small Q^2 limit, we obtain the probability,

$$P_{q\bar{q}} = F^s_{\pi^+}(Q^2)|_{Q^2=0} = \int dx \frac{d^2\mathbf{k}_\perp}{(16\pi)^3} |\Psi(x, \mathbf{k}_\perp)|^2 = \int_0^1 dx \int_0^\infty d\lambda \frac{A^2}{16\pi^2(1+\lambda)^2} \exp\left[\frac{m^2(1+\lambda)}{4(x-1)x\beta^2} \right] \times [m^2(1+\lambda) + 4x(1-x)\beta^2] \tag{24}$$

and the charged mean square radius $\langle r^2_{\pi^+} \rangle^{q\bar{q}}$ [30],

$$\langle r^2_{\pi^+} \rangle^{q\bar{q}} \approx -6 \frac{\partial F^s_{\pi^+}(Q^2)}{\partial Q^2} \bigg|_{Q^2=0} = \int_0^1 dx \int_0^\infty d\lambda \frac{3A^2}{256\pi^2 x\beta^2(1+\lambda)^3} \times \exp\left(-\frac{m^2(1+\lambda)}{4(1-x)x\beta^2} \right)(1-x)(2+4\lambda+\lambda^2) \times [8(1-x)x\beta^2 + m^2(1+\lambda)]. \tag{25}$$

In the above two equations, one may observe that the terms in the square bracket that are proportional to m^2 come from the ordinal helicity components, while the remaining terms in the square bracket are from the higher-helicity components.

The parameters in the wave function can be determined by several reasonable constraints [21]. Two constraints can be derived from $\pi \to \mu\nu$ and $\pi^0 \to \gamma\gamma$ decay amplitude [22]:

$$\int_0^1 dx \int \frac{d^2\mathbf{k}_\perp}{16\pi^3}\Psi(x, \mathbf{k}_\perp) = f_\pi/(2\sqrt{3}), \qquad \int_0^1 dx\Psi(x, \mathbf{k}_\perp = 0) = \sqrt{3}/f_\pi, \tag{26}$$

where f_π is the pion decay constant: $\langle 0|\bar{q}(0)\gamma^+\gamma_5 q(0)|P\rangle = if_\pi P^+$, the experimental value of which is 92.4 ± 0.25 MeV [31]. Experimentally the average quark transverse momentum of pion $\langle \mathbf{k}_\perp^2\rangle_\pi$ is approximately of the order $(300\text{ MeV})^2$ [32]. The quark transverse momentum of the valence state in the pion is defined as

$$\langle \mathbf{k}_\perp^2\rangle_{q\bar{q}} = \int dx \frac{d^2\mathbf{k}_\perp}{(16\pi)^3}|\mathbf{k}_\perp^2|\frac{|\Psi(x, \mathbf{k}_\perp)|^2}{P_{q\bar{q}}}, \tag{27}$$

and it should be larger than $\langle \mathbf{k}_\perp^2\rangle_\pi$. We thus could require that $\sqrt{\langle \mathbf{k}_\perp^2\rangle_{q\bar{q}}}$ has the value of a few hundreds MeV, serving as another constraint. Using the constraints and the model wave function Eq. (14), we obtain,

$$m = 310\text{ MeV}; \qquad \beta = 396\text{ MeV}; \qquad A = 0.050\text{ MeV}^{-1}, \tag{28}$$

for $\langle \mathbf{k}_\perp^2\rangle \approx (367MeV)^2$. And by using the above parameters, we obtain

$$\langle r_{\pi^+}^2\rangle^{q\bar{q}} = 0.216\text{ fm}^2, \tag{29}$$

$$P_{q\bar{q}} = P_{q\bar{q}}^{(\lambda_1+\lambda_2=0)} + P_{q\bar{q}}^{(\lambda_1+\lambda_2=\pm1)} = 0.744. \tag{30}$$

The value of $\langle r_{\pi^+}^2\rangle^{q\bar{q}}$ is in nice agreement with the ones obtained in Ref. [33,34]. In fact, we have used the same monopole ansatz as has been used in Ref. [30,34]. It is shown that the valence quark radius is smaller than the experimental value of the pion charged radius ($[0.671 \pm 0.008\text{ fm}]^2$ [31]). Therefore the valence portion of a hadron is more compact than the hadron radius. For the probability of finding the valance states in the pion, we have $P_{q\bar{q}}^{(\lambda_1+\lambda_2=0)} = 0.398$ for the usual-helicity components and $(P_{q\bar{q}}^{(\lambda_1+\lambda_2=\pm1)} = 0.346)$ for the higher-helicity states, which show that the higher-helicity components have the same importance as that of the usual-helicity components. It has been shown that even though we have added the contributions from the higher-helicity states, the probability of finding the minimal $q\bar{q}$ Fock-state in pion is still less than unity, i.e., $P_{q\bar{q}} = 0.744 < 1$. This is shown clearly in Fig. 3(a), so it is necessary to take the higher Fock states and the higher-twist terms into consideration to give a full understanding of the pion form factor at the energy region $Q^2 \to 0$. It should be noticed that if one normalizes the valence Fock-state to unity without including the higher-helicity components, then the soft and hard contributions from the valence state can be enhanced and become important inadequately. In Refs. [12,13], to fit the experimental data, the nonvalence contributions to the form factors have also been considered within the light-front dynamics.

The result for the soft contribution to the pion form factor is shown in Fig. 3. From Fig. 3(b), one may observe a quite different behavior from that of the hard contribution for the higher-helicity components ($\lambda_1 + \lambda_2 = \pm1$). In the energy region $Q^2 \lesssim 1\text{ GeV}^2$, the higher-helicity components give a large enhancement (the same order contribution) to usual-helicity ($\lambda_1 + \lambda_2 = 0$) components and after that the higher-helicity components' contributions will decrease with the increasing Q^2. At about $Q^2 \sim 4\text{ GeV}^2$, the higher-helicity components' contributions become negative and as a result, the net soft contribution will then decrease fast with the increasing Q^2, which tends to zero at about $Q^2 \sim 16\text{ GeV}^2$.

We show the combined results that come from the hard-scattering part and from the soft part for the pion form factors $Q^2F_\pi(Q^2)$ in Fig. 4, where for comparison, the experimental data [35] and the well-known asymptotic behavior for the leading-twist pion form factor have also been shown. It is shown that the soft contribution is less important as $Q^2 >$ a few GeV^2, since we have taken the correct normalization condition Eq. (30) and considered the suppression effect from the higher-helicity components. One may observe that our present result for the pion form factor is lower than the experimental data, it is reasonable since we have not taken the higher-twist effects and the higher order corrections into consideration. The next-to-leading order correction will give about ~20%–30% [17] extra contributions to the pion form factor, while the twist-3 contributions are comparable with the leading-twist contributions in a large intermediate energy region (~ 1–40 GeV) [16][1].

[1]The twist-3 contribution is model-dependent, if we take the wave function with a better end-point behavior, then the twist-3 contributions can be greatly suppressed [36].

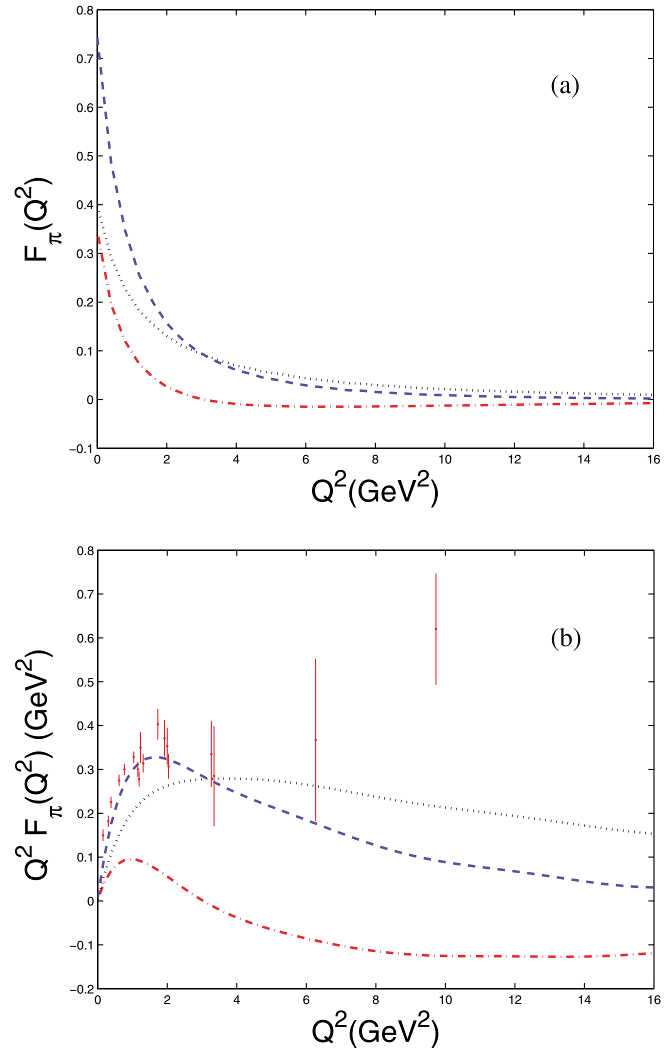

FIG. 3 (color online). The soft contribution to the pion form factor. The upper is for the pion form factor $F_\pi(Q^2)$, while the lower is for $Q^2F_\pi(Q^2)$, where the contribution comes from all the helicity components are shown in dashed line, the contribution from the ordinal helicity component $\lambda_1 + \lambda_2 = 0$ is shown in dotted line and the contribution from the higher-helicity components $\lambda_1 + \lambda_2 = \pm 1$ is shown in dashed-dotted line. The experimental data is taken from [35].

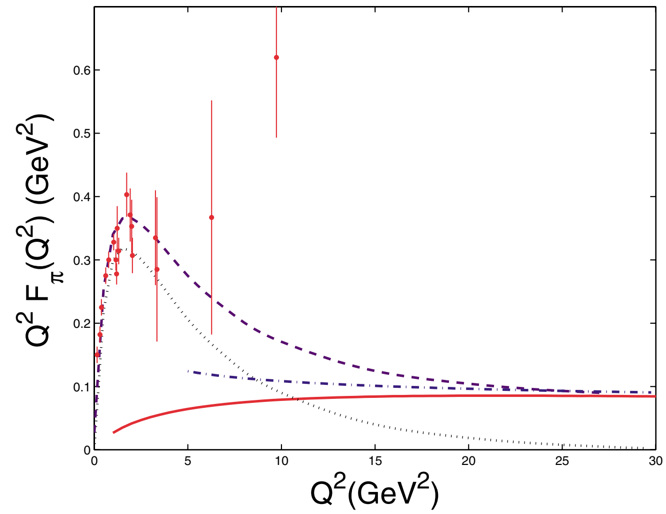

FIG. 4 (color online). The combined results for the pion form factors $Q^2F_\pi(Q^2)$. The solid line stands for the contribution from the hard part, the dotted line stands for the contribution from the soft part, the dashed line is the total Pion form factors and the dashed-dotted line is the usual asymptotic result. The experimental data are taken from [35].

V. SUMMARY AND CONCLUSION

In this paper, the transverse momentum effects and the higher-helicity contributions to the pion form factor are systematically studied based on the LC framework and the k_T factorization formalism. Both collinear and k_T factorization are the fundamental tools for applying PQCD to the pion form factor since they can separate the calculable perturbative contributions from the nonperturbative parts that can be absorbed into the bound-state wave functions. The k_T factorization theorem has been widely applied to various processes and the k_T factorization theorem for exclusive processes in PQCD has been proved by M. Nagashima and H. N. Li. Thus it provides a scheme to take the dependence of the parton transverse momentum k_T into account. Reference [3] shows that the end-point singularity can be cured by resuming the resultant double logarithms $\alpha_s \ln^2 k_T$ into a Sudakov form factor and then the PQCD analysis can make sense. In fact, the Sudakov effects have small effects for the pion form factor in the region where experimental data is available. We note that there is k_T dependence in the wave function in the k_T factorization, and it generates much larger effects than the Sudakov suppression to the hard-scattering amplitude in the present experimental Q^2 region. Our results show that it is substantial to take k_T dependence in the wave function into account.

The LC formalism provides a convenient framework for the relativistic description of the hadron in terms of quark and gluon degrees of freedom, and the application of PQCD to exclusive processes has mainly been developed in this formalism. In the present paper, we have given a consistent treatment of the pion form factor within the LC PQCD framework, i.e., both the wave function and the hard interaction kernel are treated within the framework of LC PQCD. Taking into account the spin-space Wigner rotation, one may find that there are higher-helicity components ($\lambda_1 + \lambda_2 = \pm 1$) in the LC spin-space wave function besides the usual-helicity components ($\lambda_1 + \lambda_2 = 0$). We have studied the higher-helicity components' contributions to the hard part and the soft part of the pion form factor by using the LC PQCD approach with the parton's transverse momentum

k_T included. We find that the asymptotic behavior of the hard-scattering amplitude for the higher-helicity components including the transverse momentum in the quark propagator is of order $1/Q^4$ which is the next to leading order contribution compared with the contribution coming from the ordinary helicity component, but it can give sizable contributions to the pion form factor at the intermediate energies.

In order to compare our predictions with the present experimental data, we need to know the contributions from the soft part. As an example, we have considered the soft contributions to the pion form factor with a reasonable wave function in the LC framework. Our results show that the soft contributions from the higher-helicity components have a quite different behavior from that of the hard-scattering part and have the same order contribution as that of the usual-helicity ($\lambda_1 + \lambda_2 = 0$) components in the energy region ($Q^2 \lesssim 1$ GeV^2). As $Q^2 > 1$ GeV^2, the higher-helicity components' contributions will decrease with the increasing Q^2. At about $Q^2 \sim 4$ GeV^2, the higher-helicity components' contributions become negative and as a result the net soft contributions to the pion form factor will then decrease with the increasing Q^2, which tends to zero at about $Q^2 \sim 16$ GeV^2. Thus the soft contribution is less important in the intermediate energy region. Although the soft contributions are purely nonperturbative and model-dependent, our results show that the calculated prediction for the pion form factor should take the k_T dependence in the soft and hard parts into account beside including the higher order contributions. Therefore, one needs to keep the transverse momentum in the next leading order corrections and to construct a realistic k_T dependence in the hadronic wave function in order to derive more exact prediction to the pion form factor in k_T factorization.

ACKNOWLEDGMENTS

We would like to thank Dr. F. G. Cao, Dr. J. Cao, Dr. H. N. Li and Dr. B. Q. Ma for useful discussions. This work was supported in part by the Natural Science Foundation of China (NSFC).

APPENDIX: INTEGRATION FORMULA

The error function is defined as

$$Erf(x) = \frac{2}{\sqrt{\pi}} \int_0^x e^{-t^2} dt. \tag{A1}$$

An important property for the error function is $\lim_{x\to\infty} Erf(x) = 1$.

Second we list some useful formula that are needed for integrating over the azimuth angle of the momenta $\mathbf{k}_\perp$ and $\mathbf{l}_\perp$ and then reduce the integration dimension from six to four. And the remaining four dimensional integration can be done numerically.

By using polarization coordinate, we have

$$[d\mathbf{k}_\perp^2][d\mathbf{l}_\perp^2] = kldkdld\theta d\rho/(16\pi^3)^2, \tag{A2}$$

where k, l and θ, ρ are the module and azimuth angle of $\mathbf{k}_\perp$ and $\mathbf{l}_\perp$ respectively. By using the following formula, the integration over the azimuth angle can be done analytically.

$$f_1(A, B) = \int_0^{2\pi} \frac{d\theta}{A + B\cos(\theta)} = \frac{2\pi}{\sqrt{(A+B)(A-B)}}, \tag{A3}$$

$$\begin{aligned} f_2(A, B) &= \int_0^{2\pi} \frac{\cos(\theta) d\theta}{A + B\cos(\theta)} \\ &= \frac{2\pi}{B}\left[1 - \frac{A}{\sqrt{(A+B)(A-B)}}\right], \end{aligned} \tag{A4}$$

$$\begin{aligned} f_3(A, B) &= \int_0^{2\pi} \frac{\sin(\theta) d\theta}{A + B\cos(\theta)} = 0, \\ f_4(A, B) &= \int_0^{2\pi} \int_0^{2\pi} \frac{\cos(\theta - \rho) d\theta d\rho}{A + B\cos(\theta)} = 0 \end{aligned} \tag{A5}$$

$$f_5(A, B, C) = \int_0^{2\pi} \int_0^{2\pi} \frac{\cos(\theta - \rho) d\theta d\rho}{A + B\cos(\theta) + C\cos(\rho)}, \tag{A6}$$

where A, B and C are functions that are free from θ and ρ. The result for the function f_5 is very complicated and for simplicity its explicit form will not be listed here. However, by adding a small component $[BC\cos(\theta) \times \cos(\rho)]$ (for the integration we need to deal with, we have $BC \ll A$, which corresponding to $\mathbf{k}_\perp \cdot \mathbf{l}_\perp \ll \mathbf{q}_\perp^2$), it can be solved approximately,

$$\begin{aligned} f_5(A, B, C) &\approx \int_0^{2\pi} \int_0^{2\pi} \frac{\cos(\theta - \rho) d\theta d\rho}{[A + B\cos(\theta)][A + C\cos(\rho)]} \\ &= f_2(A, B) f_2(A, C). \end{aligned} \tag{A7}$$

There one may notice that under the present approximation, the actual azimuth angle, i.e., α, for $\mathbf{q}_\perp$ will not affect the final integrated results due to the fact that after integration over θ and ρ, it will always accompanied by a factor $[\cos(\alpha)^2 + \sin(\alpha)^2] \equiv 1$.

After integrating over the azimuth angle, we can change the integration over the radius of $\mathbf{k}_\perp$ and $\mathbf{l}_\perp$ to two variables η_1 and η_2 that are within the range of (0.1) through the relation

$$|\mathbf{k}_\perp| = Q(1-x)\eta_1/2, \qquad |\mathbf{l}_\perp| = Q(1-y)\eta_2/2. \tag{A8}$$

The relation is so choosing as to insure that all the quantities in the radical sign obtained by doing the azimuth angle integration are always positive.

[1] G. P. Lepage, S. J. Brodsky, T. Huang, and P. B. Mackezie, in *Particles and Fields*, Proceedings of the Banff Summer Institute on Particle Physics, Banff, Alberta, Canada, 1981 2, edited by A. Z. Capri and A. N. Kamal (Plenum, New York, 1983), p. 83.
[2] G. P. Lepage and S. J. Brodsky, Phys. Rev. D **22**, 2157 (1980); **24**, 1808 (1981).
[3] H. N. Li and G. Sterman, Nucl. Phys. **B381**, 129 (1992); J. Botts and G. Sterman, Nucl. Phys. **B325**, 62 (1989).
[4] M. Nagashima and H. N. Li, Phys. Rev. D **67**, 014019 (2003).
[5] A. Szczepaniak, C. R. Ji, and A. Radyushkin, Phys. Rev. D **57**, 2813 (1998).
[6] C. R. Ji, A. Pang, and A. Szczepaniak, Phys. Rev. D **52**, 4038 (1995).
[7] F. G. Cao, J. Cao, T. Huang, and B. Q. Ma, Phys. Rev. D **55**, 7107 (1997).
[8] O. C. Jacob and L. S. Kisslinger, Phys. Rev. Lett. **56**, 225 (1986); Phys. Lett. B **243**, 323 (1990); L. S. Kisslinger and S. W. Wang, Nucl. Phys. **B399**, 63 (1993).
[9] L. S. Kisslinger, H. M. Choi, and C. R. Ji, Phys. Rev. D **63**, 113005 (2001).
[10] W. Schweiger, Nucl. Phys. (Proc. Suppl.) **108**, 242 (2002).
[11] V. Anisovich, D. Melikhov, and V. Nikonov, Phys. Rev. D **52**, 5295 (1995).
[12] B. L. G. Bakker, H. M. Choi, and C. R. Ji, Phys. Rev. D **63**, 074014 (2001).
[13] J. P. B. C. de Melo, T. Frederico, E. Pace, and G. Salme, Nucl. Phys. **A707**, 399 (2002).
[14] F. Schlumpf, Phys. Rev. D **50**, 6895 (1994).
[15] V. M. Braun, A. Khodjamirian, and M. Maul, Phys. Rev. D **61**, 073004 (2000).
[16] F. G. Cao, Y. B. Dai, and C. S. Huang, Eur. Phys. J. C **11**, 501 (1999); A. Szczepaniak and A. G. Williams, Phys. Lett. B **302**, 87 (1993); Z. T. Wei and M. Z. Yang, Phys. Rev. D **67**, 094013 (2003).
[17] R. D. Field, R. Gupta, S. Otto, and L. Chang, Nucl. Phys. **B186**, 429 (1981); E. Braaten and S. M. Tse, Phys. Rev. D **35**, 2255 (1987); E. P. Kadantseva, S. V. Mikhailov, and A. V. Radyushkin, Yad. Fiz. **44**, 507 (1986); Sov. J. Nucl. Phys. **44**, 326 (1986); N. G. Stefanis, W. Schroers, and H. C. Kim, Eur. Phys. J. C **18**, 137 (2000).
[18] B. Q. Ma and T. Huang, J. Phys. G **21**, 765 (1995).
[19] S. W. Wang and L. S. Kisslinger, Phys. Rev. D **54**, 5890 (1996).
[20] S. J. Brodsky, in *Summer Institute on Particle Physics, SLAC, Stanford, California, 1979* (SLAC Report No. SLAC-PUB-2447, 1979); G. P. Lapage and S. J. Brodsky, Phys. Lett. B **87**, 359 (1979).
[21] T. Huang, B. Q. Ma, and Q. X. Shen, Phys. Rev. D **49**, 1490 (1994).
[22] G. P. Lepage, S. J. Brodsky, T. Huang, and P. B. Mackenzie, *Particles and Fields* (Ref. [1]), p. 143; G. P. Lepage, S. J. Brodsky, T. Huang, and P. B. Mackenzie, *Particles and Fields* (Ref. [1]), p. 83; T. Huang, in *Proceedings of XXth International Conference on High Energy Physics, Madison, Wisconsin, 1980*, edited by L. Durand and L. G. Pondrom, AIP Conf. Proc. No. 69 (AIP, New York, 1981), p. 1000.
[23] G. P. Lepage, J. Comput. Phys. **27**, 192 (1978).
[24] V. L. Chernyak and A. R. Zhitnitsky, Nucl. Phys. **B201**, 492 (1982); Phys. Rep. **112**, 173 (1984); Nucl. Phys. **B246**, 52 (1984); T. Huang, X. D. Xiang, and X. N. Wang, Chin. Phys. Lett. **2**, 67 (1985); Phys. Rev. D **35**, 1013 (1987).
[25] S. Gottlieb and A. S. Kronfeld, Phys. Rev. Lett. **55**, 2531 (1985); Phys. Rev. D **33**, 227 (1986); G. Martinelli and C. T. Sachrajda, Phys. Lett. B **217**, 319 (1989); D. Daniel, R. Gupta, and D. G. Richards, Phys. Rev. D **43**, 3715 (1991).
[26] P. Korll and M. Raulfs, Phys. Lett. B **387**, 848 (1996).
[27] V. M. Braun and I. E. Filyanov, Z. Phys. C **44**, 157 (1989); T. Huang and Q. X. Shen, Z. Phys. C **50**, 139 (1991); C. E. Carlson and F. Gross, Phys. Rev. D **36**, 2060 (1987).
[28] H. N. Li, Phys. Rev. D **48**, 4243 (1993); J. Botts and G. Sterman, Nucl. Phys. **B381**, 129 (1989).
[29] S. D. Drell and T. M. Yan, Phys. Rev. Lett. **24**, 181 (1970).
[30] F. Cardarelli *et al.*, Phys. Lett. B **332**, 1 (1994).
[31] Particle Data Group, K. Hagiwara *et al.*, Phys. Rev. D **66**, 010001 (2002).
[32] See, e.g., W. J. Metcalf *et al.*, Phys. Lett. B **91**, 275 (1980).
[33] T. Huang, Nucl. Phys. (Proc. Suppl.) **7**, 320 (1989).
[34] F. Cardarelli *et al.*, Phys. Rev. D **53**, 6682 (1996).
[35] L. J. Bebek *et al.*, Phys. Rev. D **9**, 1229 (1974); C. N. Brown *et al.*, *ibid.* **8**, 92 (1973); J. Volmer *et al.*, Phys. Rev. Lett. **86**, 1713 (2001).
[36] T. Huang and X. G. Wu, hep-ph/0408252.